Metallomics

PAPER

View Article Online
View Journal | View Issue

Cite this: *Metallomics*, 2018, **10**, 1430

The type 4 metallothionein from *Brassica napus* seeds folds in a metal-dependent fashion and favours zinc over other metals†

Agnieszka Mierek-Adamska,[ab] Grażyna B. Dąbrowska[a] and Claudia A. Blindauer*[b]

Received 27th June 2018,
Accepted 13th August 2018

DOI: 10.1039/c8mt00161h

rsc.li/metallomics

The problem of handling zinc in the cell is of great importance because zinc is an indispensable micronutrient involved in most physiological processes in all living organisms. Moreover, our understanding of mechanisms governing the discrimination between micronutrients and toxic metals on the level of individual proteins to the whole-organism level is incomplete. Metallothioneins are able to bind heavy metal ions, and roles in zinc homeostasis have been proposed. Here, we have studied the *in vitro* and *in vivo* metal-binding abilities of *Brassica napus* type 4 metallothionein (BnMT4) and its expression in germinating seeds in response to metal treatment. Our studies on the regulation of *MT4* expression by metals at early stages of ontogenic development have revealed for the first time that the mRNA levels of *BnMT4* were elevated in response to cadmium and zinc. Given this unexpected metalloregulation, and the dramatic differences in protein folding as detected by ^{1}H NMR spectroscopy, we suggest that the BnMT4 protein may not only have a role in zinc homeostasis in early ontogenesis, but also the potential to discriminate between zinc and cadmium, perhaps *via* differential recognition of Cd- and Zn-complexes by cellular components involved in protein turnover.

Significance to metallomics

Correctly populating every metalloprotein with the right metal in the cell is indisputably crucial to the health and survival of all organisms. However, our understanding of the molecular mechanisms underlying discrimination between metals in biological systems is incomplete. Our research considers the *in vitro* properties of copper–, cadmium– and zinc–metallothionein complexes combined with *in vivo* analysis. Therefore, it provides not only evidence for metal-dependent protein folding but also insight into the possible role of this process in the cell.

Introduction

A significant part of agricultural land is deficient in zinc[1] and it is estimated that over 30% of the world's population is at risk of zinc malnutrition (www.who.org). The effects of Zn deficiency are profound and all-encompassing, because a given proteome of a higher eukaryote consists of *ca.* 10% of zinc-requiring proteins.[2] In animals and humans, almost all systems including the immune, central nervous and reproductive systems are affected by insufficient zinc intake.[3] In plants, more than 1200 proteins contain zinc including carbonic anhydrase critical for carbon fixation,[4] and therefore zinc deficiency leads to reduced growth, low photosynthetic efficiency, delay in flowering and decreased crop yields.[5] The total amount of zinc accumulated in seeds has a significant impact on the early vegetative growth of wheat seedlings[6] and the size and number of produced grains.[7] Also the seed zinc content of *Brassica napus* (rapeseed, canola) affects the growth of seedlings and their zinc uptake, especially under zinc deficiency conditions.[8] In wheat, barley and rice, Zn is localised mainly in the embryo, and also in the aleurone layer and endosperm,[9–12] whereas in endospermless *B. napus* seeds, zinc is accumulated mainly in cotyledons. During germination, its amount increases in the radicle, the most intensively growing tissue.[13] The detailed chemical speciation of zinc in seeds remains to be determined.[14] Recent work revealed that phytate is not the main storage form of zinc in rice seeds, since the distribution pattern of Zn differs from

[a] *Department of Genetics, Faculty of Biology and Environmental Protection, Nicolaus Copernicus University, Lwowska 1, 87-100 Toruń, Poland*
[b] *Department of Chemistry, University of Warwick, Coventry CV4 7AL, UK. E-mail: C.Blindauer@warwick.ac.uk; Tel: +44-(0)2476-528264*

† Electronic supplementary information (ESI) available. See DOI: 10.1039/c8mt00161h

that of phosphorus.[11] Similarly, in barley grains zinc seems to be bound to peptides and/or proteins rather than to phytate. These peptides/proteins remain to be identified; however, a part of accumulated Zn is coordinated by proteins containing thiol groups.[15]

Type 4 metallothioneins (MTs) are thiol-rich proteins present in abundant quantities in seeds of both mono- and dicotyledons, and their role as zinc/metal chelators has been proposed.[16,17] They belong to a large super-family of low-molecular-weight (<10 kDa), cysteine-rich proteins able to bind heavy metal ions with a d^{10} configuration, and are found throughout all kingdoms of life.[18,19] The first plant metallothionein (pMT) discovered was an early cysteine-labelled (E_c) protein isolated in a Zn-bound form from wheat germs.[20] Plant MTs are much more diverse in terms of length, number and arrangement of Cys residues than MTs from species of other kingdoms, and hence, they were classified into four main types, types 1–3 and type 4, also known as type E_c.[21–23] The expression of *pMTs* is affected by many endo- and exogenous stimuli including metal ions, reactive oxygen species, phytohormones, and the presence of microorganisms. Moreover, *pMT* expression is dependent on the phase of plant development, is tissue-specific and varies depending on the type of *pMT*.[23–26] *pMT4* expression in most angio- and gymnosperms is restricted to developing and mature seeds and declines rapidly after the start of germination.[17,27–31] The most likely main function of pMT4s is the storage of zinc in seeds and its distribution to nascent Zn-requiring proteins during germination.[17,32] However, *pMT4* is also expressed in young and mature leaves and sheaths of rice[33] and in leaves of the desiccation-tolerant resurrection plant *Xerophyta humilis*.[34] Here, the expression of *pMT4* is dehydration-upregulated and rehydration-downregulated, which may imply that pMT4 has physiological functions beyond micronutrient homeostasis.

Most studies concerning pMTs have been restricted to genes and their mRNA, and thus, knowledge about the structural and functional properties of pMT proteins is limited, although a few labs including that of Silvia Atrian have begun to remedy this lack of knowledge. One reason for scarce data is a high tendency for proteolytic degradation of pMTs during isolation, especially from native sources.[35] So far, the only pMT isolated directly from plant material in amounts sufficient for further characterisation has been the wheat E_c protein.[20,36] Equally, the solution NMR structures of its two domains, from the recombinantly expressed protein, remain the only 3D structures available for pMTs.[37,38] pMT4s comprise three cysteine-rich sections separated by two short Cys-free stretches, thus differing from other types of pMTs, which have Cys residues grouped into two regions, separated by a Cys-free stretch of variable length. Wheat E_c, irrespective of whether isolated from wheat embryos[20,36] or produced recombinantly in *E. coli*,[39] binds predominantly six zinc ions in two domains: the N-terminal γ-domain containing a Zn_2Cys_6 cluster, and a C-terminal domain with 11 Cys and 2 His residues that together bind 4 Zn(II) ions. NMR studies revealed that this domain contains a mononuclear $ZnCys_2His_2$ site; this site and the γ-domain Zn_2Cys_6 cluster are unprecedented features for MTs.[37,38,40]

The current report focuses on the dicot rapeseed, one of the most widely cultivated oil-plants. Its seeds are used for production of high-value food oil, biofuels and also protein-rich by-products for animal feed. Only a few studies regarding rapeseed MTs have been published so far;[30,41–45] all of these studies were limited to the mRNA level and only two of them concern also a type 4 MT.[30,45]

Agricultural land might easily be contaminated with cadmium through fertilization with cadmium-rich phosphate fertilizers. Cadmium and zinc share similar physical and chemical properties[46] and toxic effects of cadmium on plants are mainly caused by the displacement of essential metals by cadmium from a variety of biological ligands.[47] The folding of the wheat E_c protein depends on the bound metal and has been hypothesised to promote selective accumulation of essential zinc in the developing embryo over toxic cadmium.[48] Inspired by the postulated role for pMT4s in metal discrimination and reports on elevated cadmium accumulation in rapeseed,[49] we studied *BnMT4* expression in *B. napus*, the metal-binding properties and protein folding of the metallated recombinant BnMT4 protein, and its ability to confer tolerance to Zn, Cd, and Cu when expressed heterologously in *E. coli*.

Experimental

Plant materials and heavy metal ion treatment

Seeds from *B. napus* winter variety Kronos (AgroBras, Poland) were surface-sterilized in a mixture of 30% hydrogen peroxide and 96% ethanol in a 1 : 1 ratio (v/v) for 5 min and rinsed with sterile water for 30 min. The seeds were placed in Petri dishes on sterile filter paper moistened with 6 mL of sterile water (control) or 6 mL of 500 μM $ZnSO_4$, 250 μM $CuSO_4$ or 250 μM $CdSO_4$, respectively. The seeds were incubated in the dark at 26 °C and material was collected after 3, 12, 24 and 48 hours after the start of seed imbibition, frozen in liquid nitrogen, and stored at −80 °C.

Total RNA isolation and reverse transcription reaction

Total RNA isolation was performed using TRI-Reagent (Sigma-Aldrich, Poland) according to the manufacturer's protocol. The integrity of RNA was checked on 1% agarose gels in TAE (Tris/acetate/EDTA, pH 8.3) buffer with ethidium bromide (EtBr).

For the reverse transcription (RT) reaction, the following mixture of a total volume of 14.5 μL was prepared: 3 μg of total RNA, 0.5 μg of oligo$(dT)_{18}$ primer and 1 μL of 10 mM dNTPs. The mixture was incubated at 65 °C for 5 min, and then at 0 °C for 2 min. After that 40 U of RNase inhibitor, 4 μL of 5× RT Buffer and 200 U of RevertAid™ Premium Reverse Transcriptase (Thermo Scientific, MA, USA) were added. The reaction was performed at 50 °C for 30 min, and then stopped at 85 °C for 5 min. The cDNA was stored at −20 °C.

BnMT4 expression analysis

A *BnMT4* cDNA clone was obtained as reported previously (GenBank accession number JX103202.1).[30] Semi-quantitative

RT-PCR (sqRT-PCR) forward and reverse primers specific for *BnMT4* were as follows: 5′-GAAGAAAAAGAGCGAGGTAAAA-3′ and 5′-CACCCATTCCCAAGGTATGT-3′. The 5S rRNA (*Bn5S*) transcript level was used as an internal standard: forward primer 5′-AGTCGCACAAATCGTGTCTG-3′ and reverse primer 5′-TCCATGCTCTCAGCATCAAC-3′. The PCR reaction mixture includes single-stranded cDNA as a template, 0.4 μL of 10 μM forward and reverse primers, 0.4 μL of 10 mM dNTPs, 2 μL 10× buffer and 1.25 U of Opti*Taq* DNA polymerase (EURx, Poland) in a total volume of 20 μL. The thermal cycling conditions were as follows: 95 °C for 30 s, 51 °C (*BnMT4*) or 55 °C (*Bn5S*) for 40 s, 72 °C for 40 s for 26 cycles (*Bn5S*) or 28 cycles (*BnMT4*). PCR products were sequenced to confirm that specific fragments were amplified (Genomed, Poland). PCR products were separated on 2% agarose gels in TAE buffer with EtBr and their quantity was estimated by densitometric measurements using ImageGauge 3.46 software (FujiFilm, Japan).

Expression and purification of the recombinant BnMT4 protein

The coding region for *BnMT4* was amplified by PCR on cDNA using sequence-specific primers containing *Nde*I and *Xho*I restriction sites: forward 5′-AAACATATGGCAGACATAGGCAAAGG-3′ and reverse 5′-AAACTCGAGCTAAGCGGCACAAGAGGCG-3′. The PCR product was ligated with the pET21a bacterial expression vector (Novagen, Germany) and the pET-*BnMT4* construct was checked by sequencing (GATC Biotech AG, Germany).

BnMT4 was overexpressed in *E. coli* Rosetta 2(DE3)pLysS (Novagen). Overnight cultures of transformed *E. coli* cells were diluted (1 : 100, v/v) with LB medium containing 50 μg mL^{-1} ampicillin and 34 μg mL^{-1} chloramphenicol. Protein expression was induced by 0.5 mM isopropyl-β-D-thiogalactopyranoside (IPTG) at an optical density at 600 nm (OD_{600}) of *ca.* 0.6–0.7 in the presence of 0.5 mM $ZnSO_4$, 0.3 mM $CdSO_4$, or 0.1 mM $CuSO_4$. Bacteria were grown for a further 4–5 h at 37 °C and harvested by centrifugation. Cell pellets were resuspended in sonication buffer (4 mL per gram of wet mass of cells; 50 mM Tris, 100 mM KCl, 3 mM DTT, 1 mM metal ions, 0.5% Triton X-100, pH 8.5) and sonicated. The supernatant was separated from cell debris by centrifugation and was subjected to chemical precipitation with an ice-cold mixture of ethanol and chloroform (100 : 8, v/v).[50] The precipitated protein was dissolved in 20 mM NH_4HCO_3 buffer, filtrated (0.2–0.4 μm, Minisart®) and purified by FPLC (GE Healthcare Äkta Purifier, GE Healthcare, UK) using a size exclusion column (HiLoad 16/60 Superdex 75, Amersham Biosciences, UK) equilibrated with 20 mM NH_4HCO_3 buffer. The elution of the protein was monitored by measuring absorbances at 220 and 280 nm. All fractions were analysed for metal and sulfur contents by inductively-coupled plasma optical emission spectroscopy (ICP-OES, Optima 5300 DV, Perkin-Elmer, UK; *vide infra*), and selected fractions were also analysed on SDS-PAGE gels. Proteins were resolved on precast 4–15% Mini-PROTEAN®TGX™ Gel (Bio-Rad, UK) in TGS (Tris/glycine/SDS, pH 8.3; Bio-Rad) buffer and visualised by silver staining. The protein concentration was determined by measuring the S content by ICP-OES or by measuring the thiol content using Ellman's reaction[51] after demetallation by EDTA.

Elemental analysis

The S, Zn, Cd and Cu contents in all samples were analysed by ICP-OES. Mixed-element calibration standards were prepared gravimetrically in the 0.2–5.0 ppm range from commercial stocks (TraceCERT, Sigma-Aldrich). All samples and standards were prepared in 0.1 M HNO_3 (ultrapure 70% HNO_3 prepared in-house by sub-boiling point distillation).

Spectrometric and spectroscopic analysis of BnMT4

MT-containing fractions were pooled, desalted (Sephadex G-25, PD-10 desalting column, GE Healthcare) with 10 mM NH_4HCO_3 buffer and concentrated to 20–30 μM (Amicon Ultra-4 3000 Da MWCO) prior to analysis by electrospray ionisation (ESI) time-of-flight mass spectrometry (micrOTOF, Bruker Daltonics, Germany). The parameters were as follows: temperature of the ESI source: 468 K, mass spectral voltage parameters: 210 V – capillary exit, 450 V – hexapole RF, 1:70 V – skimmer, 1:19 V – hexapole. The samples in 10 mM NH_4HCO_3 and 10% MeOH were directly infused into the spectrometer using a syringe pump with a flow rate of 240 μL h^{-1}. Data were recorded for 2 min in positive mode over an *m*/*z* range of 500–3000. Spectra were averaged, smoothed and analysed using Data Analysis 4.0 software (Bruker Daltonics).

Proton-dependent loss of Zn(II) or Cd(II) ions bound to BnMT4 was analysed by UV-vis spectroscopy using a Cary 50 Bio UV-visible spectrophotometer (Varian, CA, USA) in the 200–400 nm range at room temperature. The samples (7–10 μM in 1 mM Tris buffer pH 7.89) were placed in a quartz cuvette and were titrated with dilute HCl (0.05–0.5 M, ∼1–2 μL) and UV-spectra were recorded. The pHs of the samples were measured using a benchtop meter (HANNA Instruments, UK) with BioTrode (Hamilton, NV, USA).

^{1}H NMR spectroscopy

For 1D and 2D ^{1}H NMR spectroscopy, Cd(II)–BnMT4 (950 μM) and Zn(II)–BnMT4 (880 μM) were prepared in 20 mM NH_4HCO_3 with 10% D_2O (v/v). NMR spectra were recorded at 298 K on a Bruker Avance 700 Ultrashield™ spectrometer with a TCI cryoprobe operating at 700.24 MHz for ^{1}H. The Cd(II)–BnMT4 sample was titrated with microlitre additions of diluted HCl, and 1D ^{1}H NMR spectra were recorded between pH 8.09 and 3.07. 2D ^{1}H TOCSY and NOESY data were acquired for samples of Cd(II)–BnMT4 at pH 5.2 and Zn(II)–BnMT4 at pH 6.6, in each case at 298 K, with 4k datapoints in F2 and 512 datapoints in F1. Data were apodised using a shifted sinebell function, and Fourier-transformed with 2k × 2k datapoints. In all cases, water suppression was achieved using excitation sculpting with gradients.[52]

Metal tolerance assays in bacteria

E. coli strain BL21(DE3) cells were transformed with an empty pET21a vector (control) or the pET-*BnMT4* construct. Overnight cultures of transformed *E. coli* were diluted (1 : 100, v/v) in LB medium supplemented with 50 μg mL^{-1} ampicillin, grown until OD_{600} reached *ca.* 0.6 and diluted again to OD_{600} *ca.* 0.2. At this point, expression of the BnMT4 protein was induced by

IPTG at a final concentration of 0.1 or 0.3 mM, and metal ions were added to final concentrations of 0.25 or 0.5 mM $ZnSO_4$, 0.1 or 0.25 mM $CdSO_4$, and 0.075 or 0.165 mM $CuSO_4$. Bacterial cells were collected every hour for seven hours, and the OD_{600} was measured. The growth rate of bacterial cultures, expressed as the slope of the linear proportion of the growth curve, was calculated using Microsoft Excel.

Statistical analyses

Statistical analyses were performed using PAST3.10 software.[53] ANOVA (analysis of variance) followed by Tukey's honestly significant difference test were used to determine significant differences between means. For the differences $p < 0.05$ (*) or $p < 0.01$ (**) was considered significant.

Results and discussion

Expression of *BnMT4* during seed germination in the presence of heavy metal ions

The expression of *MTs* in several plant species is induced by metal ions;[21] however, most of such studies have been limited to seedlings or vegetative parts of plants and thus only the expression of type 1–3 *pMTs* was examined.[54,55] Based on work demonstrating that during imbibition the mRNA levels of E_c significantly increased in mature wheat embryos in the presence of abscisic acid (ABA) but not zinc,[27] it has been generally assumed that the expression of *pMT4s* is not influenced by metal ion levels. More recently, *AtMT4a* and *AtMT4b* expression was shown to be highly induced in ABA-treated siliques. Treatment with Zn did not change the expression levels, but slight induction was observed after treatment with Cd;[17] therefore, the metal-responsiveness of *pMT4* genes is little studied, may differ between plant species and thus warrants investigation.

Germination is a crucial process in the life cycle of higher plants that determines all subsequent stages of growth and development and for crop plants also future yields; hence, we tested the effects of metals on the mRNA levels of *BnMT4* in germinating seeds of *B. napus* exposed to three heavy metals: cadmium, copper or zinc (Fig. 1). Transcripts of *BnMT4* in seeds germinating in water decreased during germination (Fig. 1) and were undetectable in 6-day-old seedlings.[30] The *BnMT4* mRNA level appeared slightly increased (*ca.* 1.3-fold difference) in response to all three metals at the 3rd and 12th hours of imbibition; however, the differences were not statistically significant. During the subsequent 12 hours the *BnMT4* mRNA level remained unchanged in control and Cd-treated seeds and decreased in seeds exposed to Cu and Zn, but the difference was significant only for Cu-treated seeds – almost 3-fold lower than that in the control. Between the first and the second day of germination in seeds exposed to Cu, the mRNA level of *BnMT4* was marginally reduced, but remained high in seeds treated with Cd and Zn – 4.4- and 2.4-fold higher than that in the control, respectively. In Cd-treated seeds, no decrease in the *BnMT4* expression was observed over the entire period, while in the presence of Zn and Cu the *BnMT4* transcript level gradually decreased (Fig. 1).

In animals it was demonstrated that the metal-dependent upregulation of *MT* expression is mediated by metal-responsive elements (MREs) with the core sequence 5′-TGCRCNC-3′, and MRE-binding transcription factor-1 (MTF-1).[56] MRE-like sequences have been identified in the promoters for type 1–3 *pMTs*,[57–59] but appear to be absent in the promoters of type 4 *pMTs* investigated so far. However, some novel putative regulatory elements mediating the response to metals have been identified in the promoter regions of *pMTs*, *e.g.* in green algae,[60] bean,[61] rice[62–64] or oil palm.[65] *In silico* analysis of the putative promoter region of *BnMT4* using the PlantCARE database[66] revealed the presence of several regulatory elements, but none of them were related to heavy metals. However, manual analysis identified previously described plant-specific putative *cis*-elements conferring

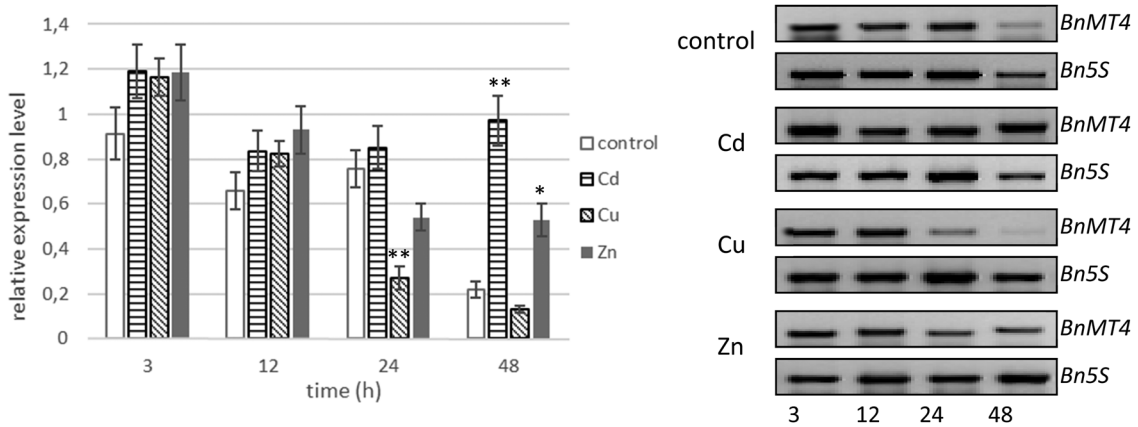

Fig. 1 Expression of rapeseed *BnMT4* in germinating seeds in response to metal treatment. Total RNAs were isolated from seeds after 3, 12, 24 and 48 h after the start of imbibition. Seeds treated with water (white bars) served as a control. The left-hand side shows relative expression levels expressed as the ratio of the densitometric measurement of the *BnMT4* RT-PCR product to the 5S rRNA RT-PCR product (*Bn5S*) (means from three independent experiments ± SE). Asterisks indicate significant differences (*$p < 0.05$, **$p < 0.01$) between the control and metal-treated seeds at a particular time point.

heavy-metal responsiveness (Fig. S1, ESI†). Therefore, it is possible that metal-ion responsive elements are present in the promoters of *pMT4* genes. We also note that the observed effects may not necessarily result from *de novo* gene expression, but could relate to the differential stabilisation of the already existing mRNA stored in mature seeds.

Metal-binding capacity of the BnMT4 protein

The predicted amino acid sequence of BnMT4 shows the highest similarity to sequences of MT4 from *Brassica oleracea* (XP_013627462.1) and *Brassica rapa* (XP_009134020.1), with 98% and 95% identities, respectively. Moreover, BnMT4 shares 79% identical amino acids with *Arabidopsis thaliana* MT4a (NP_001189730.1) and 80% with AtMT4b (NP_179905.1). The similarity to E_c-1 from monocotyledonous wheat is significantly lower (50% identities), but the number and positions of cysteine and histidine residues are fully conserved; this is, with very few exceptions, generally true for flowering plants (Fig. 2).[23]

Adopting the general approach pioneered by the Atrian and Capdevila team in Barcelona,[67] metal-to-protein stoichiometries of metal–BnMT4 complexes were analysed using the recombinant BnMT4 protein (without any point mutations or artificial purification tags) produced in *E. coli* cultured in media supplemented with Cd(II), Cu(II) and Zn(II), respectively. After purification under conditions that preserve metal–MT complexes, the metal contents were analysed using ICP-OES, and detailed qualitative metal speciation data were obtained using native ESI-MS (Table 1, Fig. 3 and 4 and Fig. S2, Tables S1 and S2, ESI†). The N-terminal methionine residue was in each case cleaved, a common feature for proteins synthesised in *E. coli*.[68] The molar Zn-to-protein ratio in the purified Zn(II)–BnMT4 samples was 6.2 ± 0.5, with no other metals detected. The 6 : 1 stoichiometry was also corroborated by the predominant species observed in ESI-MS spectra at native pH. Its neutral mass of 8716.11 Da corresponds to Zn_6BnMT4 (Fig. 3A). In contrast, when BnMT4 was expressed in the Cd- or Cu-enriched media, significant amounts of Zn were also detected (Table 1). The molar Cd-to-BnMT4 ratio was 5.9 ± 0.5 (Table 1), in agreement with the predominant Cd_6BnMT4 species detected by ESI-MS (Fig. 3C). Consistent with the detection of 0.3 molar equivalents of Zn(II) in the purified protein, ESI-MS spectra of Cd(II)–BnMT4 complexes also revealed the presence of Zn_1Cd_5BnMT4, together with minor quantities of seven- and eight-metal species (Fig. 3C). Acidification of Zn(II)– and Cd(II)–BnMT4 yielded the apo-form with a neutral mass of 8336.10 ± 0.35 Da (calculated 8467.54 Da for the full-length protein and 8336.35 Da for the protein with the N-terminal methionine residue cleaved, *cf.* the sequence in Fig. 2) as major species (Fig. 3B and D, respectively).

Table 1 Metal stoichiometry of the recombinant BnMT4 protein determined by elemental analysis and major metal–MT species observed in ESI-MS. Me stands for Cu + Zn

Supplemented metal	Zn/MT	Cd/MT	Cu/MT	Metal–MT species
Zn	6.2 ± 0.5	n.d.[a]	n.d.	Zn_6
Cd	0.3 ± 0.2	5.9 ± 0.5	n.d.	Cd_6, Cd_5Zn_1
Cu (reduced aeration)	0.7 ± 0.4	n.d.	9.7 ± 0.1	Me_{12}–Me_9
Cu (normal aeration)	1.4 ± 0.4	n.d.	12.1 ± 0.5	Me_{14}–Me_8

[a] n.d.: levels were below the limit of detection.

Generally, MTs incorporate copper in their Cu(I) oxidation state, as due to their redox potentials, Cu(II) and thiols cannot coexist. Moreover, in the reducing intracellular environment, copper is predominantly in its Cu(I) form. The intracellular copper content in *E. coli* is dependent on the level of culture aeration;[67] thus, the production of BnMT4 in Cu-enriched media was performed under both normal and reduced aeration conditions, following the example of Capdevila and Atrian.[69,70] ICP-OES results demonstrate that when BnMT4 was produced at normal aeration (low Cu(I)), heterometallic complexes containing 12.1 Cu and 1.4 Zn per BnMT4 were recovered. With reduced aeration (high Cu(I)), still heterometallic complexes were present (9.7 Cu and 0.7 Zn per BnMT4, respectively), but with a considerably higher copper-to-zinc ratio (Table 1): 13.9 *vs.* 8.6 under normal aeration. It is unknown why the overall metal-to-protein ratio was reduced under low aeration conditions. Mass spectra revealed that under both culture aeration conditions BnMT4 expressed in the presence of Cu(I) yielded several coexisting metal–BnMT4 species at neutral pH (Fig. 4A and B). Although the presence of mixed-metallated species was suggested by ICP-OES results (Table 1), it is not possible in ESI-MS to unambiguously distinguish between Cu(I) and Zn(II) because of the small difference between their masses (taking into account the masses of protons to be formally

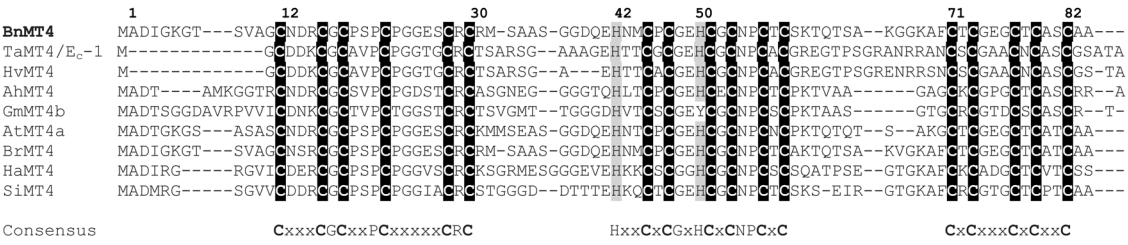

Fig. 2 Amino acid alignment of the representative members of type 4 pMTs. Conserved cysteines are marked in bold. Histidine residues with a potential metal-binding ability are highlighted in grey. The consensus sequences of Cys-rich domains were obtained through comparative analysis of numerous type 4 pMTs. GenBank accession numbers are as follows: BnMT4 *Brassica napus* (AFP57436.1, this study), TaMT4 (wheat E_c-1) *Triticum aestivum* (CAA48349.1), HvMT4 *Hordeum vulgare* (CAD88267.1), AhMT4 *Arachis hypogaea* (ABG57066.1), GmMT4b *Glycine max* (NP_001237409.2), AtMT4a *Arabidopsis thaliana* (NP_179905.1), BrMT4 *Brassica rapa* (XP_009134020.1), HaMT4 *Helianthus annuus* (XP_022016856.1), and SiMT4 *Sesamum indicum* (AAG23841.1).

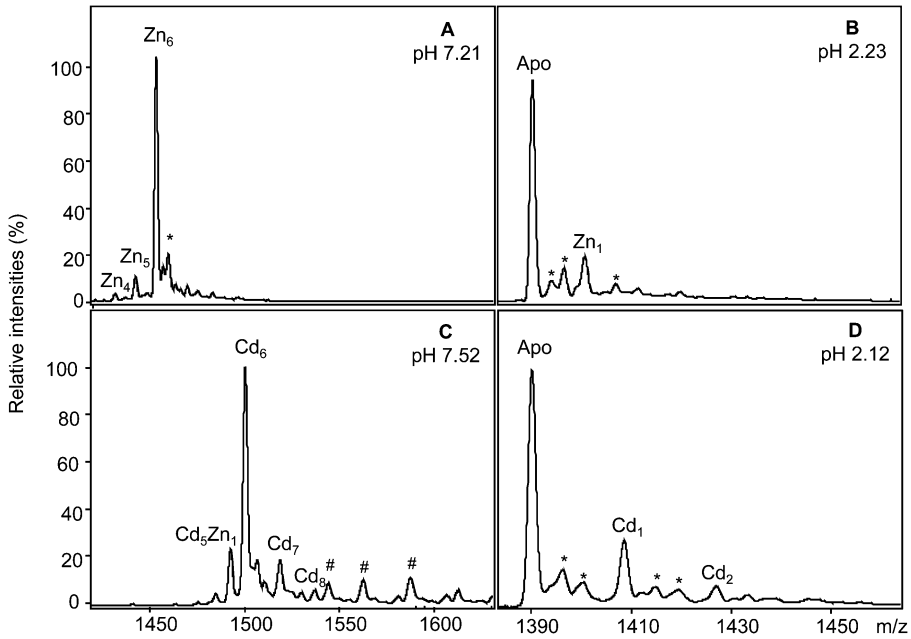

Fig. 3 Representative ESI-MS spectra (+6 charge state) of Zn- (A and B) and Cd- (C and D) BnMT4 at native pH (A and C) or acidic pH (B and D). Samples in 10 mM NH_4HCO_3, 10% MeOH, plus 2% formic acid for acidic pH samples. Likely Na^+ adducts are indicated with an asterisk, and unknown contaminants are labelled with a hash. See Table S1 (ESI†) for exact molecular masses and Fig. S2 (ESI†) for full mass spectra.

replaced to maintain charge neutrality, the mass gain for one Zn(II) ion is 63.54, and that for one Cu(I) ion is 62.55). This ambiguity is further compounded by the possibility of thiol oxidation for under-metallated species, which results in lower than calculated masses. Significantly lower than expected masses were especially prevalent in samples synthesised under normal aeration conditions (Table S2, ESI†), *i.e.* with high levels of O_2 and hence less Cu(I) and more likelihood for oxidation. Only the Me_{14} species displayed a higher than calculated mass. ESI-MS spectra of Cu(I)–BnMT4 at acidic pH showed the presence of several coexisting metallated species, but no apo-form (Fig. 4C). This is a common observation for Cu(I)-bound MT species and is due to the high thermodynamic stability of the Cu(I)–thiolate bonds.[71] Nevertheless, the reasonable agreement between the calculated and observed masses for the Cu-bound species allows the conclusion that also in this case the correct protein was isolated.

Besides wheat E_c-1, only a few other pMT4 proteins have been characterised. Recombinant *A. thaliana* MT4a and MT4b were shown to have the capacity to coordinate up to 6 Zn(II) and 6 Cd(II) ions, respectively.[23,72] The same metal stoichiometry was observed for *Helianthus annuus* MT4.[73] Recombinantly expressed MT4 from *Glycine max* (cv. Williams 82) bound 5–6 Zn(II) ions or 6 Cd(II) ions.[74] The lower Zn/protein stoichiometry is likely a consequence of this particular cultivar lacking the second, (normally) conserved His residue. Both His residues are required to form the mononuclear Zn(II) site, and the second His residue is critical for structuring the entire C-terminal domain.[48] Interestingly, for MT4 from *Sesamum indicum* and *Hordeum vulgare* expressed recombinantly in *E. coli*, unexpected poorly metallated complexes were observed – 2 Zn/SiMT4, 2 Cu/SiMT4[29] and 2.6 Zn/HvMT4, 0.19 Cu/HvMT4, and 0.12 Cd/HvMT4.[32] The lower metal/MT ratios may not only be due to the synthesis/purification approaches used but may also reflect the possible existence of partially metallated MT species *in planta*. In animals the existence of such species was confirmed, and their role as reactive oxygen species scavengers was suggested.[75] Moreover, it was proposed that (undermetallated) MTs may connect cellular redox balance and zinc metabolism.[76]

Traditional classification systems divide MTs into families based mainly on primary sequence similarities and phylogenetic relationships.[77,78] More recently, a classification system based on the metal-binding properties of each MT peptide was proposed by the Barcelona team: a stepwise gradation between strict Zn- and genuine Cu-thioneins.[67,79] Although we consider pMT4s as prime examples of Zn-thioneins,[23,48,72] the occurrence of biologically relevant copper–MT4 interactions *in planta* cannot be excluded. Tarasava *et al.*[80] have recently shown that wheat E_C-1 binds copper in a site-specific manner *in vitro* and the possible existence of mixed-metal MT4 species *in planta* was suggested. The E_C-1 protein isolated directly from wheat germs contained sub-stoichiometric amounts of copper[36] although it could not be ruled out that Cu(I) contamination occurred during purification. Nevertheless, the clean formation of the Zn_6BnMT4 species (Fig. 3A), contrasted with the observation of multiple heterometallic species when BnMT4 was produced in Cu-supplemented media (Fig. 4A, B and Table 1), is consistent with the proposition that BnMT4, similarly to other pMT4s studied to date, has clear Zn–thionein character.

pH stability of metal–BnMT4 complexes

The pH value of half-dissociation (pH(1/2)) is defined as the pH at which 50% of the initially bound metal ions have dissociated

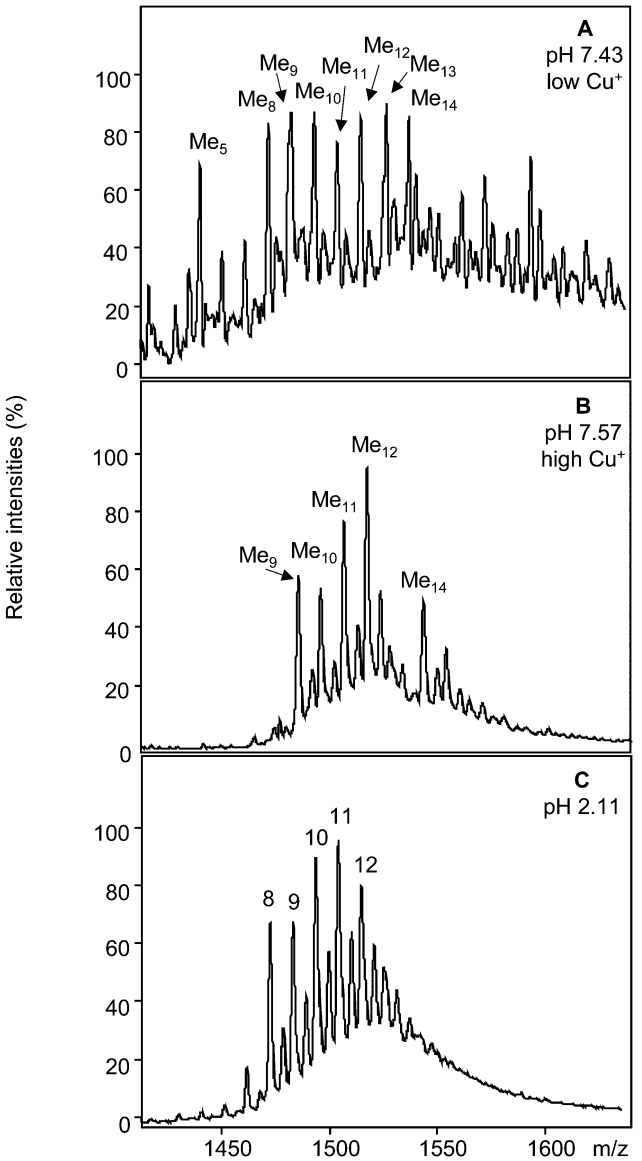

Fig. 4 Representative ESI-MS spectra (+6 charge state) of Cu-BnMT4 at native pH (A and B) or acidic pH (C) synthesized at a normal (A) or reduced (B) aeration level. Samples in 10 mM NH_4HCO_3, 10% MeOH, plus 2% formic acid for acidic pH samples. Me (A and B) stands for Zn + Cu. See Table S2 (ESI†) for exact molecular masses and Fig. S2 (ESI†) for full mass spectra.

from the MT, and is typically measured by UV-visible spectrophotometry, using the ligand-to-metal charge transfer (LMCT) bands at 230 nm (for Zn–MT, Fig. 5A) or 250 nm (for Cd–MT, Fig. 5B). The pH(1/2) is taken to correspond to the pH value of the half-maximum absorbance $1/2(A_{max} + A_{min})$. This quantity is related to the protein's affinity towards the respective metal ion and is useful for comparing metal affinities of different MTs with each other.[81] Since Cd–S bonds are much stronger than Zn–S bonds, a higher proton concentration is required to displace Cd(II) ions from MTs compared to Zn(II), and hence the pH(1/2) values for Cd-bound MTs are typically at least one pH unit lower than those for Zn-bound MTs.[71]

The pH(1/2) values for the Zn_6BnMT4 and Cd_6BnMT4 complexes were estimated from the plots of absorbance of the LMCT bands *vs.* the respective pH value (Fig. 5C and D). A value of 4.50 was obtained for Zn_6BnMT4 (Fig. 5C), similar to values obtained previously for Zn_6E_C-1 (4.53),[40] Zn_6AtMT4a (4.55) and Zn_6AtMT4b (4.56).[23] A value of 3.33 for Cd_6BnMT4 (Fig. 5D) is also almost identical to that of Cd_6E_C-1 (3.35),[40] and somewhat higher than the value of 3.1 obtained for both *Arabidopsis* MT4s.[23] As expected, both pH(1/2) and the pH at which the complete loss of the initially bound metal ions occurs are significantly lower for Cd(II)–BnMT4 than for Zn(II)–BnMT4. However, the loss of Cd(II) starts already at pH 7, indicating that some Cd(II) ions are bound quite weakly. There also appears to be a small additional step above pH 4. From the absorbance values at the start and end of the titration, it can be estimated that about 5 out of the *ca.* 6 Cd(II) ions are lost in the steep step.

The pH(1/2) values for Zn(II)- and Cd(II)-complexes of pMT4s are the lowest among pMTs, comparable to those of vertebrate MTs, which implies higher stability of metal–thiolate clusters.[22] Attempts to study BnMT4 synthesised in Cu-enriched media in the same way indicated that although a decrease of absorbance at 280 nm (LMCT band for Cu(I)) was observed (data not shown), the complete release of metal ions was not achieved within accessible pH ranges, as observed previously by ESI-MS at acidic pH (Fig. 4C). Therefore, the pH(1/2) value could not be determined.

Proton-driven demetallation of Zn(II)- and Cd(II)-BnMT4 was further studied using ESI-MS, which may inform about the fashion in which metallation/demetallation of MTs occurs (Fig. 6 and Tables S3, S4, ESI†).[82] The considerably different metal-binding behaviours of BnMT4 towards Zn(II) and Cd(II) are evident. Proton-dependent loss of Zn(II) ions occurs in a gradual fashion, with all possible species present during the pH titration (Fig. 6A–E). Zn_6BnMT4 was the most abundant species down to pH $\sim$ 5 (Fig. 6A and B), with a significant amount of the Zn_5 species also observed at pH 5.05. The decrease of the pH value to 4.48 resulted in a mixture of all species ranging from Zn_1BnMT4 to Zn_6BnMT, with Zn_4BnMT4 being narrowly the most abundant (Fig. 6C). The apo-form was the predominant species detected at pH 4.14 (Fig. 6D) and 3.50 (Fig. 6E). The metal speciation determined by ESI-MS during the proton-dependent demetallation suggests that this occurs in a largely noncooperative fashion for Zn(II)–BnMT4, *i.e.* the loss of one metal ion does not affect the affinity to the remaining metal ions, and thus, all partially metallated species have, apart from statistical effects, comparable Zn(II) affinities. Noncooperative demetallation was shown previously for Zn(II)-E_C-1 when reacted with EDTA,[83] although pH-dependent demetallation of Zn(II)-E_C led to the accumulation of a Zn_4E_c species, with virtually absent Zn_5E_C.[36] The comparable stabilities of partially metallated Zn–BnMT4 species highlights their potential for involvement in cellular Zn(II) chemistry.

In contrast, Cd_6BnMT4 (and also Cd_5Zn_1BnMT4 and Cd_7BnMT4) was stable against metal loss up to pH 5.4 (Fig. 6F and G). At pH 4.21 (Fig. 6H) a nearly equimolar mixture of Cd_5- and Cd_6BnMT4 complexes was detected. Interestingly,

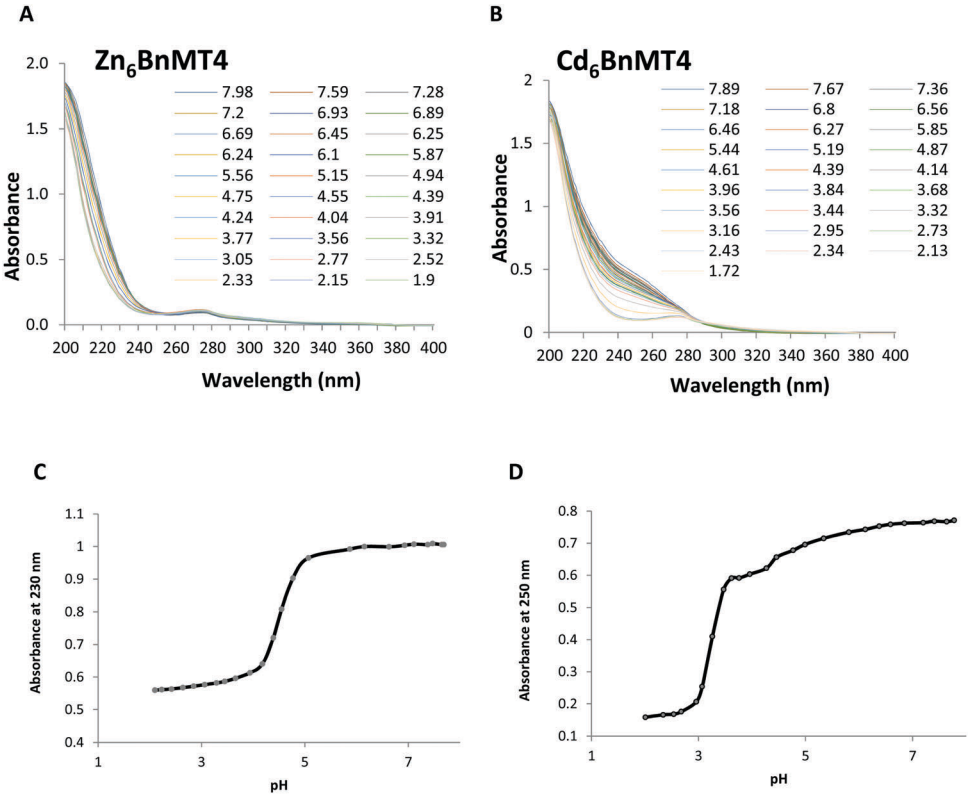

Fig. 5 Proton-dependent loss of Zn(II) or Cd(II) bound to BnMT4. The upper panels show raw UV-vis spectra of Zn_6BnMT4 (A) and Cd_6BnMT4 (B) at different pH values. (C) and (D) show plots of absorbance at either 230 nm for Zn(II)-thiolate LMCT bands (C) or 250 nm for Cd(II)-thiolate LMCT bands (D) against pH values. The lines in graphs C and D are drawn to guide the eye, and do not correspond to curve fits. The pH(1/2) values for the Zn_6BnMT4 and Cd_6BnMT4 complexes were estimated by reading from the graphs (C and D) the pH values that correspond to the $1/2(A_{max} + A_{min})$.

the Cd_5BnMT4 species was the major form observed down to pH 3.51 (Fig. 6I). The transition from Cd_5 to the apo-form occurred abruptly below this pH. At pH 3.06 the apo-form was the most abundant and only minor peaks corresponding to metallated species were observed (Fig. 6J). This abrupt loss is consistent with a certain degree of cooperativity within the Cd_5BnMT4 species. It is also noteworthy that this transition coincides with the steep drop in absorbance seen in the UV-vis data (Fig. 5D), whereas the small drop in absorbance between pH 5 and 3.5 probably corresponds to the transition from Cd_6 to Cd_5.

The persistence of the Cd_5BnMT4 species observed by ESI-MS (Fig. 6F–J) is an intriguing unprecedented behaviour for pMT4 proteins. Therefore, ^{1}H NMR spectroscopy was used to further investigate metal-dependent protein folding.

^{1}H NMR spectroscopy: effect of metals on protein folding

The majority of zinc–MTs fold equally well with either Zn(II) or Cd(II), with the notable exception of wheat E_C-1.[48] To investigate whether the nature of the bound metal impacts protein folding in BnMT4, 2D TOCSY NMR spectra of Zn_6BnMT4 and Cd_6BnMT4 were acquired (Fig. 7). The appearance of the fingerprint region of the Zn_6BnMT4 spectrum is characteristic of a well-folded protein. This assessment is corroborated by partial sequential assignment. In contrast, Cd_6BnMT4 is only partially folded, as indicated by a lower number of dispersed backbone NH resonances, and an accumulation of NH resonances in the region typical of random-coil chemical shifts (*ca.* 8.0–8.5 ppm). In this case, partial sequential assignment reveals that the N-terminal γ-domain is well-folded, whereas the absence of assignable peaks for the C-terminal domain indicates structural disorder. This parallels observations made for wheat E_C-1;[37,48] the crucial role of the mononuclear Cys_2His_2 site in metal-dependent folding – and hence folding-mediated metal-discrimination – has been highlighted.[23,48] The underlying concept for this behaviour is Pearson's principle of hard and soft acids and bases:[84] The soft cation Cd(II) prefers the softer thiolate ligands of cysteines, whereas the borderline Zn(II) shows no clear preference for either histidine nitrogen or thiolate sulfur, as demonstrated previously.[85] Thus, the $ZnCys_2His_2$ site forms and promotes order in the C-terminal domain in the presence of Zn(II) only. The site does not form with Cd(II), which results in structural disorder.

Due to this behaviour, it has so far been impossible to derive a full experimental 3D structure for a pMT4, as this requires the determination of metal-to-ligand connectivities by heteronuclear [^{1}H,^{111}Cd] or [^{1}H,^{113}Cd] NMR experiments. ESI-MS data (Fig. 6F–J) imply high relative stability of the Cd_5 species, and it was therefore of interest to explore whether this species was amenable to NMR structural studies. 1D ^{1}H NMR spectra were recorded for a

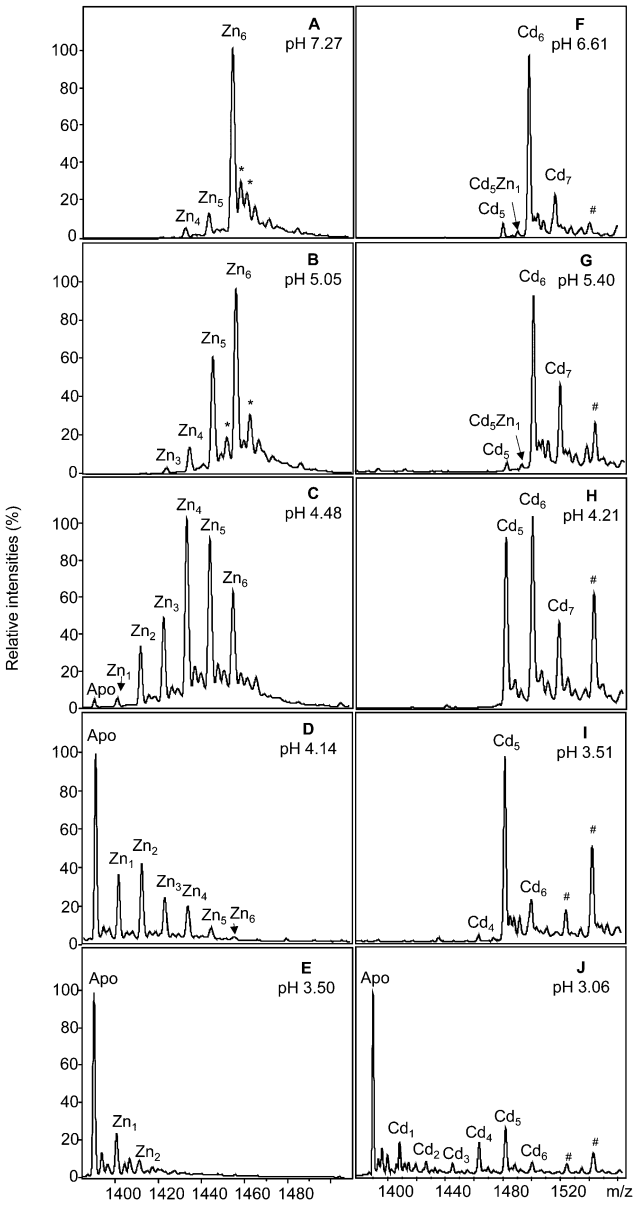

Fig. 6 Speciation of Zn(II)- and Cd(II)-BnMT4 at different pH values (10 mM NH_4HCO_3, 10% MeOH) obtained by addition of dilute formic acid. Likely Na^+/K^+ adducts are indicated with an asterisk, and the peak labelled with a hash is an unknown contaminant. See Tables S3 and S4 (ESI†) for exact molecular masses.

range of pH values (Fig. 8), as inspection of dispersion and linewidths permits a quick assessment of overall folding. No dramatic changes in chemical shifts between pH 7.1 and 5.6 were observed, which implies that there was little to no change in protein folding. According to the ESI-MS data, the Cd_6 form dominates in this pH range. At pH 5.1 and below, the more dispersed resonances (*e.g.* those at 9.45, 8.95, 7.95, 7.80 ppm – belonging exclusively to the γ-domain) start decreasing in intensity, suggesting a loss of ordered structure in the γ-domain, too. The ESI-MS data indicate a transition from the Cd_6 to the Cd_5 form in this pH range, with the Cd_5 form dominating at pH 3.8–3.5. At pH 3, most NH backbone resonances are accumulated in a broad unresolved fashion in the region expected for random coil chemical shifts, which indicates that the protein is now essentially unfolded (Fig. 8). In summary, it is likely that the Cd_5 species does not owe its persistence to a well-defined protein fold; in fact, it is likely that even the individual fold of the γ-domain may no longer be present in this metallospecies.

Metal ion tolerance of *E. coli* expressing the BnMT4 protein

The ability of BnMT4 to incorporate Zn(II), Cd(II) and Cu(I) *in vivo* (in *E. coli*) was demonstrated earlier in this study. To establish whether such binding conferred tolerance against any of the metals tested, the effect of the heterologous overexpression of *BnMT4* on the growth of *E. coli* was investigated (Fig. 9). The addition of IPTG had a negative impact on growth irrespective of whether the cells were transformed with an empty vector (pET21a) or pET-*BnMT4*. The similarity between these two results indicates that the protein itself is not toxic to *E. coli*. 0.5 mM Zn, and all concentrations of Cd or Cu also led to decreased growth, presumably due to metal toxicity. Any combination of IPTG and metal ions was also deleterious to bacterial growth, again irrespective of whether or not the protein was expressed. A direct comparison between the empty vector and pET-*BnMT4* under the same individual conditions reveals that there was no difference in growth in Cd-supplemented media. In the presence of Cu, there was a small decrease for pET-*BnMT4*, whereas only in the case of Zn, the BnMT4 expression increased the growth rate. Notably, this effect was observed even in the absence of IPTG; it is suggested that this may be due to leaky expression, and indeed, this was confirmed by SDS-PAGE (Fig. S3, ESI†).

Thus, bacteria expressing *BnMT4* showed increased tolerance only towards Zn, whilst their tolerance towards Cd was not affected, and the tolerance towards Cu was decreased in comparison to control cells expressing the empty vector. Although an increased tolerance of bacteria expressing other types of *pMTs* towards different metal ions was previously demonstrated,[86–88] the heterologous expression of GST-AtMT4a and GST-AtMT4b did not enhance their tolerance towards Zn and Cu, but only led to higher cell contents of these two metals in bacterial cells.[17] *AtMT4a* and *AtMT4b* conferred higher Cu tolerance when expressed in the yeast mutant *Δcup1* and higher Zn tolerance and accumulation when expressed in a *Δzrc1Δcot1* mutant.[89] In contrast, a *Δace1* yeast mutant (ACE1 is a copper-dependent transcription factor responsible for the activation of yeast metallothionein CUP1) overexpressing barley *MT4* showed only slightly higher tolerance towards Cu, whereas no complementation was observed in the case of a cadmium-sensitive *Δycf1* strain, lacking a vacuolar GSH-conjugated cadmium transporter.[32] The *in planta* overexpression of *AtMT4a* and *AtMT4b* led to increased contents of both Zn and Cu in seeds, but in *AtMT4a* and *ATMT4b* co-silencing lines, only the seed levels of Zn, but not Cu were reduced.[17] Ectopic expression of *AtMT4a* increased plants' tolerance towards Cu and Zn, but contrastingly only Cu accumulation was enhanced in vegetative tissues.[90]

The picture that emerges with respect to copper is that, when overexpressed in *E. coli*, yeast, or plants, type 4 MTs can contribute to copper binding and accumulation, but that this

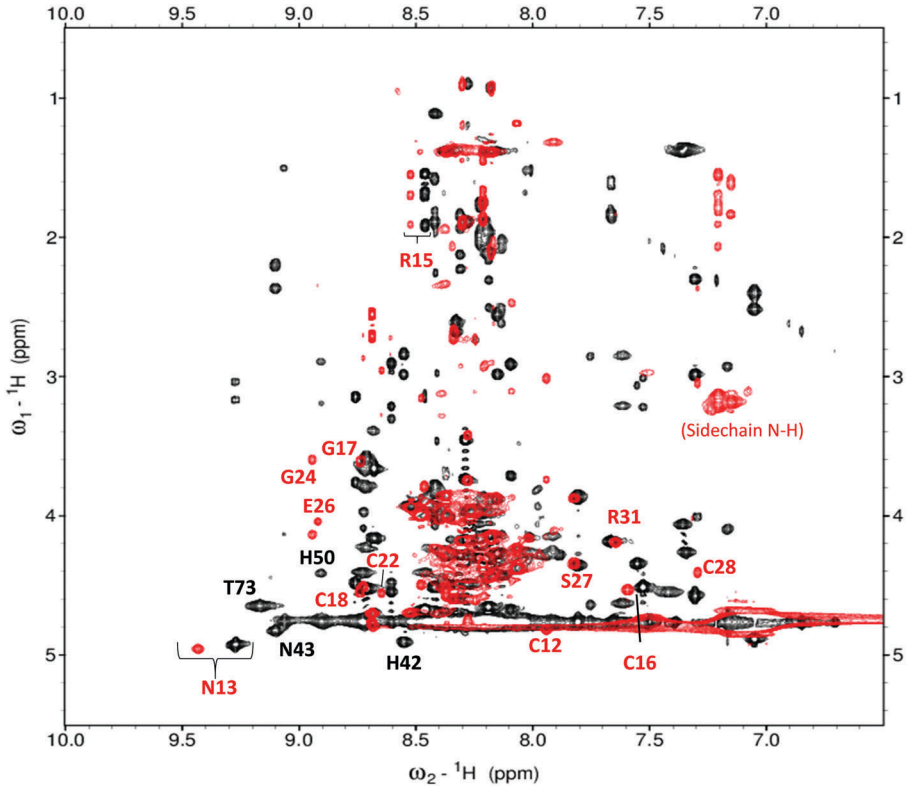

Fig. 7 Comparison of the fingerprint regions of 2D [^{1}H,^{1}H] TOCSY NMR spectra of Zn(II)-BnMT4 at pH 6.6 (black) and Cd(II)-BnMT4 at pH 5.2 (red). Samples (~0.9 mM) in 20 mM NH_4HCO_3 buffer and 10% D_2O.

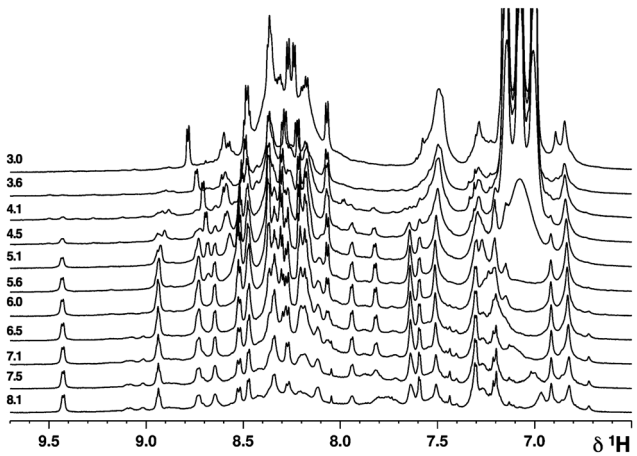

Fig. 8 Overlay of the fingerprint regions of 1D ^{1}H-NMR spectra of Cd_6BnMT4 acquired at different pH values. Samples (0.95 mM) in 20 mM NH_4HCO_3 and 10% D_2O. The strong triplet around 7 ppm visible at lower pH corresponds to the protons of the ammonium ion.

does not necessarily confer enhanced copper tolerance. This may be rationalised by considering that the MT4-bound Cu(I) may not be firmly sequestered by these proteins that have evolved to bind Zn(II), and as a consequence, Cu(I) may be released more readily and/or be redox-active when MT-bound. Furthermore, given the multitude of metallospecies formed, it is conceivable that they would be structurally disordered, as well-defined folds usually correlate with well-defined metal stoichiometry.[71] Such misfolded species are likely to be more prone to proteolysis, which would also result in the release of Cu(I). In each of these scenarios, bacterial growth would be impaired due to copper toxicity (Fig. 9). We note that in plants and their seeds, there will be other proteins, including other pMTs, to ensure the safe handling of copper.

Conclusions

In summary, the data presented in this study showed that

(i) the presence of metals during seed germination affected *BnMT4* mRNA levels (Fig. 1). The effect of copper differed from those of zinc and cadmium.

(ii) BnMT4 expressed in the presence of Cu forms a large range of mixed-metal (Cu and Zn) species (Fig. 4)

(iii) Cd_6–BnMT4, although the major metallospecies at neutral pH, is partially misfolded (Fig. 3 and 7)

(iv) BnMT4 forms a well-defined Zn_6 species with a well-ordered protein fold (Fig. 3 and 7)

(v) *BnMT4* overexpression in *E. coli* mitigated zinc toxicity, but did not confer tolerance towards either Cd or Cu (Fig. 9)

All observations are consistent with the role of BnMT4 in zinc homeostasis before and/or during germination. It is intriguing that despite the clearly demonstrated ability to strongly bind Cu and Cd, no tolerance to these metals was conferred to the

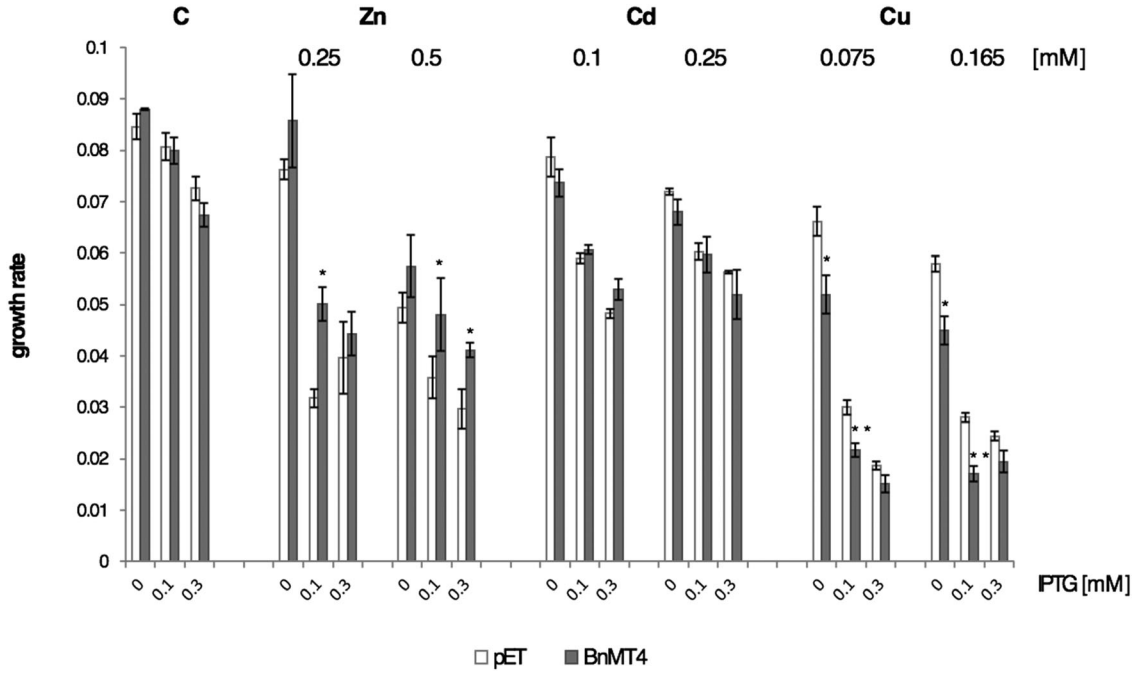

Fig. 9 Comparison of the growth of *E. coli* expressing BnMT4 (grey bars) with bacteria transformed with an empty pET vector (white bars) in the presence of Zn(II), Cd(II) and Cu(II). The *y* axis corresponds to the slopes of the bacterial growth curves that were obtained from plotting optical density against time. Media were supplemented with two different concentrations of metal ions and two concentrations of IPTG. Bacteria grown in medium without metals and with or without IPTG serve as a control (C). Data are means of three independent experiments ± SE. Asterisks indicate significant differences (*$p < 0.05$, **$p < 0.01$) between control cells and cells expressing *BnMT4* under particular conditions (metal and IPTG).

heterologous host *E. coli*. We suggest that in both cases this may be due to protein misfolding and enhanced degradation, with concomitant metal release. Based on these considerations, and particularly their dramatically different folding behaviours in the presence of Zn(II) *vs.* Cd(II), type 4 pMTs may act as metal-specific filters. In this context, metal-dependent folding of BnMT4 may lead to the preferential storage (in the maturing seed) of essential Zn over toxic Cd.

Abbreviations

ESI-MS	Electrospray ionisation mass spectrometry
ICP-OES	Inductively-coupled plasma optical emission spectroscopy
FPLC	Fast protein liquid chromatography
MTs	Metallothioneins
MRE	Metal response element

Conflicts of interest

There are no conflicts to declare.

Acknowledgements

AMA's fellowship at the University of Warwick was supported by the European Union (''Enhancing Educational Potential of Nicolaus Copernicus University in the Disciplines of Mathematical and Natural Sciences'' conducted under Sub-measure 4.1.1: Human Capital Operational Programme—Task 7 (Project No POKL.04.01.01-00-081/10)'' and a Marie Sklodowska-Curie Individual Fellowship conducted within the Horizon2020 programme (Grant No. 701492-PMTFOS)). AMA thanks Dr Hasan Tanvir Imam for his support in laboratory work. We are grateful to the University of Warwick and Nicolaus Copernicus University for financial support and use of facilities and we thank technical staff at the University of Warwick.

References

1 B. J. Alloway, Soil factors associated with zinc deficiency in crops and humans, *Environ. Geochem. Health*, 2009, **5**, 537–548.
2 C. Andreini, L. Banci, I. Bertini and A. Rosato, Zinc through the three domains of life, *J. Proteome Res.*, 2006, **5**, 3173–3178.
3 N. Roohani, Zinc and its importance for human health: an integrative review, *J. Res. Med. Sci.*, 2013, **18**, 144–157.
4 E. Andresen, E. Peiter and H. Küpper, Trace metal metabolism in plants, *J. Exp. Bot.*, 2018, **69**, 909–954.
5 S. A. Sinclair and U. Krämer, The zinc homeostasis network of land plants, *Biochim. Biophys. Acta*, 2012, **1823**, 1553–1567.
6 Z. Rengel and R. D. Graham, Importance of seed zinc content for wheat growth on zinc deficient soil. I. Vegetative growth, *Plant Soil*, 1995, **173**, 259–266.

7 Z. Rengel and R. D. Graham, Importance of seed Zn content for wheat growth on Zn deficient soil. II. Grain yield, *Plant Soil*, 1995, **173**, 267–274.
8 H. S. Grewal and R. D. Graham, Seed zinc content influences early vegetative growth and zinc uptake in oilseed rape (*Brassica napus* and *Brassica juncea*) genotypes on zinc-deficient soil, *Plant Soil*, 1997, **192**, 191–197.
9 L. Ozturk, M. A. Yazici, C. Yucel, A. Torun, C. Cekic, A. Bagci, H. Ozkan, H. J. Braun, Z. Sayers and I. Cakmak, Concentration and localization of zinc during seed development and germination in wheat, *Physiol. Plant.*, 2006, **128**, 144–152.
10 E. Lombi, E. Smith, T. H. Hansen, D. Paterson, M. D. de Jonge, D. L. Howard, D. P. Persson, S. Husted, C. Ryan and J. K. Schjoerring, Megapixel imaging of (micro)nutrients in mature barley grains, *J. Exp. Bot.*, 2011, **62**, 273–282.
11 T. Iwai, M. Takahashi, K. Od, Y. Terada and K. T. Yoshida, Dynamic changes in the distribution of minerals in relation to phytic acid accumulation during rice seed development, *Plant Physiol.*, 2012, **160**, 2007–2014.
12 B. Ajiboye, I. Cakmak, D. Paterson, M. D. de Jonge, D. L. Howard, S. P. Stacey, A. A. Torun, N. Aydin and M. J. McLaughlin, X-ray fluorescence microscopy of zinc localization in wheat grains biofortified through foliar zinc applications at different growth stages under field conditions, *Plant Soil*, 2015, **392**, 357–370.
13 K. Eggert and N. von Wirén, Dynamics and partitioning of the ionome in seeds and germinating seedlings of winter oilseed rape, *Metallomics*, 2013, **5**, 1316–1325.
14 S. Clemens, Zn and Fe biofortification: the right chemical environment for human bioavailability, *Plant Sci.*, 2014, **225**, 52–57.
15 D. P. Persson, T. H. Hansen, K. H. Laursen, J. K. Schjoerring and S. Husted, Simultaneous iron, zinc, sulfur and phosphorus speciation analysis of barley grain tissues using SEC-ICP-MS and IP-ICP-MS, *Metallomics*, 2009, **1**, 418–426.
16 I. Kranner and L. E. Colville, Metals and seeds: biochemical and molecular implications and their significance for seed germination, *Environ. Exp. Bot.*, 2011, **72**, 93–105.
17 Y. Ren, Y. Liu, H. Chen, G. Li, X. Zhang and J. Zhao, Type 4 metallothionein genes are involved in regulating Zn ion accumulation in late embryo and in controlling early seedling growth in *Arabidopsis*, *Plant, Cell Environ.*, 2012, **34**, 770–789.
18 Y. Kojima, P. A. Binz and J. H. R. Kägi, in *Metallothionein IV*, ed. C. D. Klaassen, Birkhäuser Verlag AG, Basel, 1999, pp. 3–6.
19 C. A. Blindauer and O. I. Leszczyszyn, Metallothioneins: unparalleled diversity in structures and functions for metal ion homeostasis and more, *Nat. Prod. Rep.*, 2010, **27**, 720–741.
20 B. Lane, R. Kajioka and T. D. Kennedy, The wheat-germ E_c protein is a zinc-containing metallothionein, *Biochem. Cell Biol.*, 1987, **65**, 1001–1005.
21 C. S. Cobbett and P. Goldsbrough, Phytochelatins and metallothioneins: roles in heavy metal detoxification and homeostasis, *Annu. Rev. Plant Biol.*, 2002, **53**, 159–182.
22 E. Freisinger, Plant MTs – long neglected members of the metallothionein superfamily, *Dalton Trans.*, 2008, 6663–6675.
23 O. I. Leszczyszyn, H. T. Imam and C. A. Blindauer, Diversity and distribution of plant metallothioneins: a review of structure, properties and functions, *Metallomics*, 2013, **5**, 1146–1169.
24 G. K. Zhou, Y. Xu, J. Li, L. Yang and J. Y. Liu, Molecular analyses of the metallothionein gene family in rice (*Oryza sativa* L), *J. Biochem. Mol. Biol.*, 2006, **39**, 595–606.
25 V. H. Hassinen, A. I. Tervahauta, H. Schat and S. O. Kärenlampi, Plant metallothioneins – metal chelators with ROS scavenging activity?, *Plant Biol.*, 2011, **13**, 225–232.
26 G. Dąbrowska, C. Baum, A. Trejgell and K. Hrynkiewicz, Impact of arbuscular mycorrhizal fungi on the growth and expression of gene encoding stress protein – metallothionein BnMT2 in the non-host crop *Brassica napus* L, *J. Plant Nutr. Soil Sci.*, 2014, **177**, 459–467.
27 I. Kawashima, T. D. Kennedy, T. Chino and B. G. Lane, Wheat E_c metallothionein genes. Like mammalian Zn^{2+} metallothionein genes, wheat Zn^{2+} metallothionein genes are conspicuously expressed during embryogenesis, *Eur. J. Biochem.*, 1992, **209**, 971–976.
28 W. J. Guo, W. Bundithya and P. B. Goldsbrough, Characterization of the *Arabidopsis* metallothionein gene family: tissue-specific expression and induction during senescence and in response to copper, *New Phytol.*, 2003, **159**, 369–381.
29 C. L. Chyan, T. T. Lee, C. P. Liu, Y. C. Yang, J. T. C. Tzen and W. M. Chou, Cloning and expression of a seed-specific metallothionein-like protein from sesame, *Biosci., Biotechnol., Biochem.*, 2005, **69**, 2319–2325.
30 G. Dąbrowska, A. Mierek-Adamska and A. Goc, Characteristics of *Brassica napus* L. metallothionein genes: expression in organs and during seed germination, *Aust. J. Crop Sci.*, 2013, **7**, 1324–1332.
31 M. Schiller, J. N. Hegelund, P. Pedas, T. Kichey, K. H. Laursen, S. Husted and J. K. Schjoerring, Barley metallothioneins differ in ontogenetic pattern and response to metals, *Plant, Cell Environ.*, 2014, **37**, 353–367.
32 J. N. Hegelund, M. Schiller, T. Kiche, T. H. Hansen, P. Pedas, S. Husted and J. K. Schjoerring, Barley metallothioneins: MT3 and MT4 are localized in the grain aleurone layer and show differential zinc binding, *Plant Physiol.*, 2012, **159**, 1125–1137.
33 G. K. Zhou, Y. F. Xu and J. Y. Liu, Characterization of a rice class II metallothionein gene: tissue expression patterns and induction in response to abiotic factors, *J. Plant Physiol.*, 2005, **162**, 686–696.
34 H. Collett, A. Shen, M. Gardner, J. M. Farrant, K. J. Denby and N. Illing, Towards transcript profiling of desiccation tolerance in *Xerophyta humilis*: construction of a normalized 11 k *X. humilis* cDNA set and microarray expression analysis of 424 cDNAs in response to dehydration, *Physiol. Plant.*, 2004, **122**, 39–53.
35 E. Freisinger, Structural features specific to plant metallothioneins, *JBIC, J. Biol. Inorg. Chem.*, 2011, **16**, 1035–1045.

36 O. I. Leszczyszyn, R. Schmid and C. A. Blindauer, Toward a property/function relationship for metallothioneins: histidine coordination and unusual cluster composition in a zinc-metallothionein from plants, *Proteins*, 2007, **68**, 922–935.

37 E. A. Peroza, R. Schmucki, P. Günter, E. Freisinger and O. Zerbe, The β_E-domain of wheat E_c-1 metallothionein: a metal-binding domain with a distinctive structure, *J. Mol. Biol.*, 2009, **387**, 207–218.

38 J. Loebus, E. A. Peroza, N. Blüthgen, T. Fox, W. Meyer-Klaucke, O. Zerbe and E. Freisinger, Protein and metal cluster structure of the wheat metallothionein domain γ-E(c)-1: the second part of the puzzle, *JBIC, J. Biol. Inorg. Chem.*, 2011, **16**, 683–694.

39 E. A. Peroza and E. Freisinger, Metal ion binding properties of *Triticum aestivum* E_c-1 metallothionein: evidence supporting two separate metal thiolate clusters, *JBIC, J. Biol. Inorg. Chem.*, 2007, **12**, 377–391.

40 E. A. Peroza, A. Al Kaabi, W. Meyer-Klaucke, G. Wellenreuther and E. Freisinger, The two distinctive metal ion binding domains of the wheat metallothionein E_c-1, *J. Inorg. Biochem.*, 2009, **103**, 342–353.

41 V. Buchanan-Wollaston, Isolation of cDNA clones for genes that are expressed during leaf senescence in *Brassica napus*. Identification of a gene encoding a senescence-specific metallothionein-like protein, *Plant Physiol.*, 1994, **105**, 839–846.

42 C. Hanfrey, M. Fife and V. Buchanan-Wollaston, Leaf senescence in *Brassica napus*: expression of genes encoding pathogenesis-related proteins, *Plant Mol. Biol.*, 1996, **30**, 597–609.

43 V. Buchanan-Wollaston and C. Ainsworth, Leaf senescence in *Brassica napus*: cloning of senescence related genes by subtractive hybridisation, *Plant Mol. Biol.*, 1997, **33**, 821–834.

44 H. M. Abdelmigid, Expression analysis of type 1 and 2 metallothionein genes in rapeseed (*Brassica napus* L.) during short-term stress using sqRT-PCR analysis, *Indian J. Exp. Biol.*, 2016, **54**, 212–218.

45 Y. Pan, M. Zhu, S. Wang, G. Ma, X. Huang, C. Qiao, R. Wang, X. Xu, Y. Liang, K. Lu, J. Li and C. Qu, Genome-wide characterization and analysis of metallothionein family genes that function in metal stress tolerance in *Brassica napus* L, *Int. J. Mol. Sci.*, 2018, **19**, 2181.

46 L. Tang, R. Qiu, Y. Tang and S. Wang, Cadmium-zinc exchange and their binary relationship in the structure of Zn-related proteins: a mini review, *Metallomics*, 2014, **6**, 1313–1323.

47 H. Küpper and E. Andresen, Mechanisms of metal toxicity in plants, *Metallomics*, 2016, **8**, 269–285.

48 O. I. Leszczyszyn, C. R. J. White and C. A. Blindauer, The isolated Cys_2His_2 site in E_c metallothionein mediates metal-specific protein folding, *Mol. BioSyst.*, 2010, **6**, 1592–1603.

49 R. F. Brennan and M. D. A. Bolland, Canola takes up more cadmium and phosphorus from soil than spring wheat, *J. Plant Nutr.*, 2005, **28**, 931–948.

50 M. Vašák, Large-scale preparation of metallothionein: biological sources, *Methods Enzymol.*, 1991, **205**, 39–41.

51 G. L. Ellman, Tissue sulfhydryl groups, *Arch. Biochem. Biophys.*, 1959, **82**, 70–77.

52 T. L. Hwang and A. J. Shaka, Water suppression that works. Excitation sculpting using arbitrary wave-forms and pulse-field gradients, *J. Magn. Reson., Ser. A*, 1995, **112**, 275–279.

53 O. Hammer, D. A. T. Harper and P. D. Ryan, *PAST: paleontological statistics software package for education and data analysis*, Palaeo. Electron., 2001, vol. 4, p. 9.

54 A. Kohler, D. Blaudez, M. Chalot and F. Martin, Cloning and expression of multiple metallothioneins from hybrid poplar, *New Phytol.*, 2004, **164**, 83–93.

55 Y. O. Ahn, S. H. Kim, J. Lee, H. Kim, H. S. Lee and S. S. Kwak, Three *Brassica rapa* metallothionein genes are differentially regulated under various stress conditions, *Mol. Biol. Rep.*, 2012, **39**, 2059–2067.

56 G. W. Stuart, P. F. Searle and R. D. Palmiter, Identification of multiple metal regulatory elements in mouse metallothionein-I promoter by assaying synthetic sequences, *Nature*, 1985, **317**, 828–831.

57 I. M. Evans, L. N. Gatehouse, J. A. Gatehouse, N. J. Robinson and R. R. D. Croy, A gene from pea (*Pisum sativum* L.) with homology to metallothionein genes, *FEBS Lett.*, 1990, **262**, 29–32.

58 C. A. Whitelaw, J. A. Le Huquet, D. A. Thurman and A. B. Tomsett, The isolation and characterization of the type II metallothionein-like genes from tomato (*Lycopersicon esculentum* L.), *Plant Mol. Biol.*, 1997, **33**, 503–511.

59 B. Usha, G. Venkataraman and A. Parida, Heavy metal and abiotic stress inducible metallothionein isoforms from *Prosopis juliflora* (SW) D.C. show differences in binding to heavy metals *in vitro*, *Mol. Genet. Genomics*, 2009, **281**, 99–108.

60 J. M. Quinn and S. Merchant, Two copper-responsive elements associated with the *Chlamydomonas Cyc6* gene function as targets for transcriptional activators, *Plant Cell*, 1995, **7**, 623–638.

61 X. Qi, Y. Zhang and T. Chai, Characterization of a novel plant promoter specifically induced by heavy metal and identification of the promoter regions conferring heavy metal responsiveness, *Plant Physiol.*, 2007, **143**, 50–59.

62 Y. Ren and J. Zhao, Functional analysis of the rice metallothionein gene OsMT2b promoter in transgenic Arabidopsis plants and rice germinated embryos, *Plant Sci.*, 2009, **176**, 528–538.

63 C. J. Dong, Y. Wan, S. S. Yu and J. Y. Liu, Characterization of a novel rice metallothionein gene promoter: its tissue specificity and heavy metal responsiveness, *J. Integr. Plant Biol.*, 2010, **52**, 914–924.

64 G. Dąbrowska, A. Mierek-Adamska and A. Goc, Plant metallothioneins: putative functions identified by promoter analysis *in silico*, *Acta Biol. Cracov., Ser. Bot.*, 2012, **54**, 104–120.

65 V. Omidvar, S. N. A. Abdullah, A. Izadfard, C. L. Ho and M. Mahmood, The oil palm metallothionein promoter contains a novel AGTTAGG motif conferring its fruit-specific

expression and is inducible by abiotic factors, *Planta*, 2010, **232**, 925–936.

66 V. Lescot, P. Dehais, G. Thijs, K. Marchal, Y. Moreau, Y. Van de Peer, P. Rouze and S. Rombauts, PlantCARE, a database of plant *cis*-acting regulatory elements and a portal to tools for *in silico* analysis of promoter sequences, *Nucleic Acids Res.*, 2002, **30**, 325–327.

67 O. Palacios, S. Atrian and M. Capdevila, Zn- and Cu-thioneins: a functional classification for metallothioneins?, *JBIC, J. Biol. Inorg. Chem.*, 2011, **16**, 991–1009.

68 P. H. Hirel, M. J. Schmitter, P. Dessen, G. Fayat and S. Blanquet, Extent of N-terminal methionine excision from *Escherichia coli* proteins is governed by the side-chain length of the penultimate amino acid, *Proc. Natl. Acad. Sci. U. S. A.*, 1989, **86**, 8247–8251.

69 J. Domènech, R. Orihuela, G. Mir, S. Atrian and M. Capdevila, The Cd(II)-binding abilities of recombinant *Quercus suber* metallothionein: bridging the gap between phytochelatins and metallothioneins, *JBIC, J. Biol. Inorg. Chem.*, 2007, **12**, 867–882.

70 R. Bofill, R. Orihuela, M. Romagosa, J. Domènech, S. Atrian and M. Capdevila, *Caenorhabditis elegans* metallothionein isoform specificity – metal binding abilities and the role of histidine in CeMT1 and CeMT2, *FEBS J.*, 2009, **276**, 7040–7056.

71 C. A. Blindauer, in *Binding, transport and storage of metal ions in biological cells*, ed. W. Maret and A. Wedd, Royal Soc. Chemistry, Cambridge, UK, 2014, pp. 606–665.

72 H. T. Imam and C. A. Blindauer, Differential reactivity of closely related zinc(II)-binding metallothioneins from the plant *Arabidopsis thaliana*, *JBIC, J. Biol. Inorg. Chem.*, 2018, **23**, 137–154.

73 M. Tomas, M. A. Pagani, C. S. Andreo, M. Capdevila, R. Bofill and S. Atrian, His-containing plant metallothioneins: comparative study of divalent metal-ion binding by plant MT3 and MT4 isoforms, *JBIC, J. Biol. Inorg. Chem.*, 2014, **19**, 1149–1164.

74 M. A. Pagani, M. Tomas, J. Carrillo, R. Bofill, M. Capdevila, S. Atrian and C. S. Andreo, The response of the different soybean metallothionein isoforms to cadmium intoxication, *J. Inorg. Biochem.*, 2012, **117**, 306–315.

75 W. Feng, F. W. Benz, J. Cai, W. M. Pierce and Y. J. Kang, Metallothionein disulfides are present in metallothionein-overexpressing transgenic mouse heart and increase under conditions of oxidative stress, *J. Biol. Chem.*, 2006, **13**, 681–687.

76 A. Krężel and W. Maret, Different redox states of metallothionein/thionein in biological tissue, *Biochem. J.*, 2007, **402**, 551–558.

77 N. J. Robinson, A. M. Tommey, C. Kuske and P. J. Jackson, Plant metallothioneins, *Biochem. J.*, 1993, **295**, 1–10.

78 P. A. Binz and J. H. R. Kägi, in *Metallothionein IV*, ed. C. D. Klaassen, Birkhäuser Verlag AG, Basel, 1999, pp. 7–13.

79 M. Valls, R. Bofill, R. González-Duarte, P. González-Duarte, M. Capdevila and S. Atrian, A new insight into metallothionein (MT) classification and evolution, *J. Biol. Chem.*, 2001, **276**, 32835–32843.

80 K. Tarasava, J. Loebus and E. Freisinger, Localization and spectroscopic analysis of the Cu(I) binding site in wheat metallothionein E_c-1, *Int. J. Mol. Sci.*, 2016, **17**, E371.

81 E. Freisinger, in *Metal Ions in Life Sciences*, ed. A. Sigel, H. Sigel and R. K. O. Sigel, Royal Soc. Chemistry, Cambridge, UK, 2009, vol. 5, pp. 107–153.

82 D. E. K. Sutherland and M. J. Stillman, The ''magic numbers'' of metallothionein, *Metallomics*, 2011, **3**, 444–463.

83 O. I. Leszczyszyn and C. A. Blindauer, Zinc transfer from the embryo-specific metallothionein E_c from wheat: a case study, *Phys. Chem. Chem. Phys.*, 2010, **12**, 13408–13418.

84 R. G. Pearson, Hard and soft acids and bases, *J. Am. Chem. Soc.*, 1963, **85**, 3533–3539.

85 B. A. Krizek, D. L. Merkle and J. M. Berg, Ligand variation and metal-ion binding-specificity in zinc finger peptides, *Inorg. Chem.*, 1993, **32**, 937–940.

86 A. Zhigang, L. Cuijie, Z. Yuangang, D. Yejie, A. Wachter, R. Gromes and T. Rausch, Expression of *BjMT2*, a metallothionein 2 from *Brassica juncea*, increases copper and cadmium tolerance in *Escherichia coli* and *Arabidopsis thaliana*, but inhibits root elongation in *Arabidopsis thaliana* seedlings, *J. Exp. Bot.*, 2006, **57**, 3575–3582.

87 Y. O. Kim, D. H. Patel, D. S. Lee, Y. Song and H. J. Bae, High cadmium-binding ability of a novel *Colocasia esculenta* metallothionein increases cadmium tolerance in *Escherichia coli* and tobacco, *Biosci., Biotechnol., Biochem.*, 2011, **75**, 1912–1920.

88 E. Dundar, G. D. Sonmez and T. Unver, Isolation, molecular characterization and functional analysis of OeMT2, an olive metallothionein with a bioremediation potential, *Mol. Genet. Genomics*, 2015, **290**, 187–199.

89 W. J. Guo, M. Meetam and P. B. Goldsbrough, Examining the specific contributions of individual *Arabidopsis* metallothioneins to copper distribution and metal tolerance, *Plant Physiol.*, 2008, **146**, 1697–1706.

90 I. D. Rodríguez-Llorente, P. Pérez-Palacios, B. Doukkali, M. A. Caviedes and E. Pajuelo, Expression of the seed-specific metallothionein *mt4a* in plant vegetative tissues increases Cu and Zn tolerance, *Plant Sci.*, 2010, **178**, 327–332.